Inactivation of liver X receptor β leads to adult-onset motor neuron degeneration in male mice

Sandra Andersson*†, Nina Gustafsson*, Margaret Warner*†, and Jan-Åke Gustafsson*†‡

Departments of *Medical Nutrition and †Biosciences, Karolinska Institute, Novum, 141 86 Huddinge, Sweden

Contributed by Jan-Åke Gustafsson, January 25, 2005

Male mice with inactivated liver X receptor (LXR) β suffer from adult-onset motor neuron degeneration. By 7 months of age, motor coordination is impaired, and this condition is associated with lipid accumulation and loss of motor neurons in the spinal cord, together with axonal atrophy and astrogliosis. Several of these features are reminiscent of the neuropathological signs of chronic motor neuron disease such as amyotrophic lateral sclerosis. Because the LXRs are important for cholesterol and lipid metabolism, we speculate that absence of LXRβ leads to pathological accumulation of sterols and lipids that may themselves be neurotoxic or may modulate intracellular pathways and thereby predispose motor neurons to degeneration.

amyotrophic lateral sclerosis | spinal cord

The liver X receptors (LXRs; LXRα and LXRβ) are ligand-activated nuclear receptors that play a crucial role in the regulation of cholesterol and sterol trafficking between tissues. The two LXRs share 78% amino acid sequence identity in both their DNA- and ligand-binding domains (1), and appear to bind their cognate ligands, endogenous oxysterols, with similar affinities. The most potent endogenous ligands are 22(R)-hydroxycholesterol, 24(S)-hydroxycholesterol, 24(S), 25-epoxycholesterol, and 27-hydroxycholesterol (2–6).

LXR knockout mice have confirmed that LXRs are important for controlling cholesterol transport, absorption and elimination, and fatty acid metabolism. Accumulation of lipids occurs in the liver when LXRα knockout mice (LXR$\alpha-/-$) are challenged with a high-cholesterol diet (7). Expression of several hepatic genes involved in cholesterol and fatty acid homeostasis is impaired, and this results in a block of catabolism and excretion of cholesterol and an increase in dietary cholesterol uptake. LXRβ knockout mice (LXR$\beta-/-$) maintain their resistance to dietary cholesterol (8), indicating a more prominent role of LXRα than LXRβ as a hepatic sensor for lipid and cholesterol metabolites. The physiological functions of LXRβ have not yet been elucidated.

LXRβ is broadly expressed in the developing and adult rodent brain (9, 10). We have previously shown that LXRs are important in the brain: in LXR$\alpha\beta$ double-knockout mice, the lateral ventricles are closed and ependymal cells lining the ventricles accumulate lipid droplets. There is also neuronal loss and astrocyte proliferation, particularly in the substantia nigra and globus pallidus (11). These morphological changes could be caused by an alteration of the secretion and filtration of cerebrospinal fluid or to defects in elimination of cholesterol from the brain.

In humans, $\approx$25% of the total amount of the cholesterol in the body resides within the brain. In mammals, >95% of the cholesterol content in the brain is derived from *in situ* biosynthesis, and there is little, if any, uptake of cholesterol from plasma (12, 13). The reason for this occurring is probably the inability of lipoprotein particles that mediate the intercellular transport of sterols and other lipids, to pass through the tight junctions between the endothelial cells in brain capillaries, the so-called blood–brain barrier (14). In adults, cholesterol synthesis in the brain exceeds the need, and cholesterol has to be excreted from the brain. Conversion of cholesterol to 24(S)-hydroxycholesterol is thought to be an important mechanism for efflux of cholesterol from the CNS (15). In contrast to cholesterol, 24(S)-hydroxycholesterol can cross the blood–brain barrier and enter the general circulation. Approximately two-thirds of the cholesterol efflux from the CNS occurs after hydroxylation by cholesterol 24-hydroxylase (CYP46A1); the mechanism through which the remaining one-third of brain cholesterol is excreted is unclear (16, 17). None of the major cholesterol transport proteins such as low-density lipoprotein receptor, scavenger receptor class B type I, or ATP-binding cassette transporter A1 seem to be involved (18).

In adults, synthesis of cholesterol in the spinal cord is 5-fold higher than it is in the cerebrum or cerebellum, yet the concentration of cholesterol in the spinal cord is only 2-fold higher than it is in these two brain regions (18). This finding indicates that the spinal cord must have a high capacity for excretion of cholesterol but the expression of neuronal CYP46A1 is less abundant in the spinal cord than brain, and presumably, does not play an important role in the export of cholesterol from the spinal cord (19). The major mechanism by which cholesterol is excreted from the spinal cord is still not known.

In the present study, we show that male LXR$\beta-/-$ mice suffer from impaired motor coordination associated with lipid accumulation and loss of motor neurons in the spinal cord, with several features reminiscent of neuropathological signs of chronic motor neuron disease such as amyotrophic lateral sclerosis (ALS).

Materials and Methods

Animals. LXR$\beta-/-$ mice were generated by gene targeting as described (8). All mice used in our study have been fully backcrossed for 10 generations to C57BL/6 background. Mice were housed with a regular 12-h light/12-h dark cycle and given free access to water and standard rodent chow. The local ethical committee for animal experiments, Stockholm Södra Djurförsöksetiska Nämnd, reviewed and approved the experiments following established guidelines for animal care.

Rotating Rod Test. At 7 months of age, both male and female LXR$\beta-/-$ and WT mice were placed onto a rod of 1.5 cm in diameter that was rotated at a constant velocity of 15 rpm. The retention time of mice on the rod was recorded, and mice staying for 90 sec were taken from the rod and recorded as 90 sec. Five trials per day were given for 5 consecutive days. In each genotype group, 10–13 mice were used and means were compared by Student's *t* test.

Wire-Hanging Test. Seven-month-old male mice were placed with their forepaws gripping the middle of a 50-cm-long horizontal

Abbreviations: LXR, liver X receptor; LXR$\alpha-/-$, LXRα knockout mice; LXR$\beta-/-$, LXRβ knockout mice; CYP46A1, cholesterol 24-hydroxylase; ALS, amyotrophic lateral sclerosis; SOD1, Cu/Zn superoxide dismutase; ABCG5/G8, ATP-binding cassette transporters G5 and G8; GFAP, glial fibrillary acidic protein; ChAT, choline acetyltransferase.

‡To whom correspondence should be addressed. E-mail: jan-ake.gustafsson@mednut.ki.se.

metallic wire (2 mm in diameter) that was suspended between two rods, 30 cm above a foam mattress. The performance of the mice was observed for 30 sec in four separate trials. The latency to fall was recorded and the ability to grip the wire was scored according to the following system: 0, fell off; 1, hung onto the wire with two forepaws; 2, in addition to 1, attempted to climb onto the wire; 3, hung onto the wire with two forepaws and one or both hind paws; 4, hung onto the wire with all four paws with tail wrapped around the wire; and 5, escaped to one of the supports. Student's *t* test was used to compare means of WT and LXR$\beta-/-$ mice.

Neuromuscular Junctions. Biceps femoris muscles from 7-month-old male mice were dissected, pinned in mild stretch, and fixed by immersion in 4% paraformaldehyde (in 0.1 M PBS, pH 7.4) overnight. After rinsing in PBS, muscles were dehydrated in 20% sucrose-PBS and frozen on dry ice. Muscles were cryosectioned at 30 μm, and sections were stained first with tetramethylrhodamine-conjugated α-bungarotoxin (1:40, Molecular Probes) for 30 min. After rinsing in PBS, sections were labeled with anti-synapsin I (1:200, Calbiochem) in 3% BSA for 12 h at 4°C to mark synaptic terminals. Secondary antibody was FITC-labeled donkey anti-rabbit (1:100, Jackson ImmunoResearch, West Grove, PA). VECTASHIELD mounting medium (Vector Laboratories) was used to coverslip the sections. Stained sections were examined under a Nikon Eclipse E1000 fluorescence microscope (Nikon, Tokyo). Motor endplates (red) were scored as innervated if there was an overlap with the axon terminal (green) or as denervated if the endplate was not associated with an axon. Each muscle was sectioned exhaustively so that most neuromuscular junctions could be evaluated. Mean counts for WT and LXR$\beta-/-$ mice were compared by Student's *t* test.

Neuropathology. Seven-month-old male mice were deeply anesthetized with avertin, and brains and vertebral columns were removed and postfixed overnight in 4% paraformaldehyde (0.1 M PBS, pH 7.4). The spinal cords were dissected out, and tissue specimens were processed for paraffin embedding. Sections of brain and spinal cord were cut in coronal orientation on a rotary microtome at 6 μm and examined after staining with 0.25% thionin (Nissl staining). Luxol fast blue was used to stain myelin. The paraffin sections were treated with xylene and 95% alcohol and then stained overnight in 0.1% Luxol fast blue at 37°C, followed by rinses in 95% ethanol and distilled water to remove excess blue stain. The sections were differentiated by using lithium carbonate and counterstained with Mayer's hematoxylin (Merck, Darmstadt, Germany). Lipid deposits were revealed by staining with Oil red O on 20-μm cryosections as described (20).

For immunohistochemical studies, the tissue sections were deparaffinized, rehydrated through graded alcohol, and processed for antigen retrieval by boiling in 10 mM citrate buffer (pH 6.0) for 20 min. Sections were then incubated in 0.5% H_2O_2 for 30 min to quench endogenous peroxidases, followed by 10% normal horse or goat serum and 0.5% Triton X-100 in PBS for 30 min to permeabilize and to block unspecific binding. Sections were then incubated with goat anti-glial fibrillary acidic protein (GFAP) antibody (C-19, 1:300, Santa Cruz Biotechnology) or goat anti-choline acetyltransferase (ChAT), (1:500, Chemicon) or mouse anti-calbindin (1:1000, Sigma) in 3% BSA/0.3% Triton X-100 for 12 h at 4°C. Sections were then incubated with biotinylated rabbit anti-goat or goat anti-mouse IgG (1:300, Vector Laboratories) for 1 h at room temperature, and then the avidin–biotin complex was mixed according to manufacturer's instructions (Vector Laboratories) for 1 h at room temperature. After every step, sections were washed with PBS for 45 min. Staining was developed with 3, 3′-diaminobenzidine (DAKO). All visualization and capturing was performed by using a Nikon Eclipse E1000 microscope with an attached Nikon DMX 1200 digital camera.

In the lateroventral horns of L1 segments of the spinal cord, the number of motor neurons was evaluated by counting large ChAT-positive cells having a distinct nucleus. Astroglia were counted as GFAP-positive cells having a distinct star-like shaped cell body. Cells were counted in alternate serial sections and at least 100–200 motor neurons were counted for each spinal cord specimen. This sample size has been repeatedly shown to produce coefficients of error within reasonable limits for a biological system (21). Every fourth section was analyzed, and thus a total of 15–20 slides were counted per spinal cord specimen. Quantification was made with IMAGEPRO PLUS software (Media Cybernetics, Silver Spring, MD). Mean counts for each group were compared by Student's *t* test.

Ventral Roots. Ventral nerve roots in the paraffin specimen of spinal cords were visualized by staining with 1% aqueous Toluidine blue, rinsed, and coverslipped. The mean diameter of axon interiors was measured with IMAGEPRO PLUS software. Means were compared by Student's *t* test.

Western Blot of Cerebellar Extracts. Seven-month-old male mice were asphyxiated with CO_2, and the cerebellum was dissected out and immediately frozen in liquid nitrogen. All of the following tissue handling was performed at 4°C. The specimens were homogenized twice for 1 min each with a polytron in lysis buffer (5 ml/g tissue) containing 10 mM Tris (pH 7.5), 1.5 mM EDTA, 5 mM sodium molybdate, 10 mM KCl, 1 mM α-monothioglycerol, and protease inhibitor mixture according to manufacturer's instructions (Roche Diagnostics, Mannheim, Germany). The homogenates were sonicated twice for 10 sec and centrifuged for 1 h at 100,000 $\times$ *g*. The supernatant fractions were collected and 5% glycerol was added. The protein content was measured by Bio-Rad protein assay with BSA as standard. Fifty micrograms of protein was mixed with a sample-loading buffer and resolved on 16% Tris-glycine precast gel (Invitrogen). Transfer to polyvinylidene difluoride membrane (Amersham Pharmacia Bioscience, Uppsala) was performed by electroblotting at 150 mA for 1 h. The membrane was then incubated in blocking solution containing 10% fat-free milk and 0.1% Nonidet P-40 in PBS for 2 h at room temperature. Incubation with rabbit anti-calretinin (1:1,000, Swant, Bellinzona, Switzerland) or mouse anti-calbindin (1:3,000, Sigma) was performed in blocking solution overnight at 4°C. For loading control, rabbit anti-α-tubulin was used (H-300, 1:300, Santa Cruz Biotechnology). After washing, secondary peroxidase-conjugated goat anti-rabbit or rabbit anti-mouse antibody (1:5,000, Sigma) was applied in blocking solution for 1 h at room temperature. After washing, detection with an enhanced chemiluminescence ECL kit (Amersham Pharmacia) was performed.

Results

Impaired Motor Performance in Male LXR$\beta-/-$ Mice. At 7 months of age, both male and female LXR$\beta-/-$ and WT mice were tested for their performance on a rota-rod (Fig. 1). There were five trials per day for 5 consecutive days. The LXR$\beta-/-$ mice performed better for each day as the trial went on. They learned as quickly as the WT mice, but for the male LXR$\beta-/-$ mice, the ability to stay on the rod was of significantly shorter duration than WT mice for all 5 days (day 1: WT, 31 $\pm$ 18 sec; LXR$\beta-/-$, 12 $\pm$ 5 sec; $P = 0.001$; day 2: WT, 23 $\pm$ 10 sec; LXR$\beta-/-$, 11 $\pm$ 6 sec; $P = 0.002$; day 3: WT, 53 $\pm$ 22 sec; LXR$\beta-/-$, 21 $\pm$ 12; $P < 0.001$; day 4: WT, 48 $\pm$ 18 sec; LXR$\beta-/-$, 22 $\pm$ 15 sec; $P < 0.001$; and day 5: WT 64 $\pm$ 16 sec; LXR$\beta-/-$, 33 $\pm$ 24 sec; $P = 0.002$).

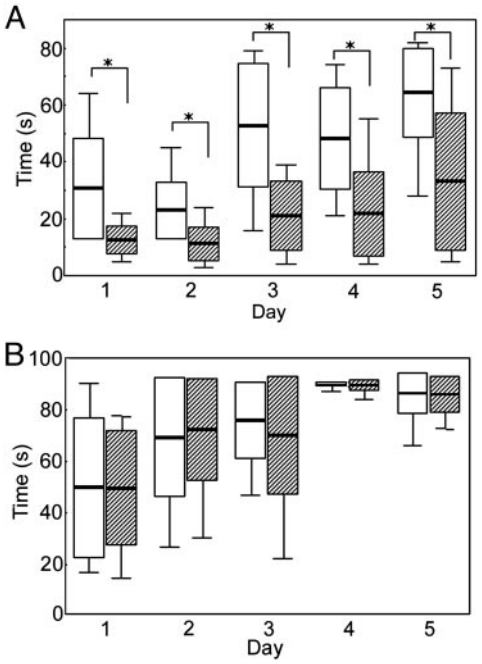

Fig. 1. Box plot of rota-rod performance in 7-month-old mice. Five trials per day were given for 5 consecutive days. The retention time of mice on the rod was recorded, and mice staying for 90 sec were taken from the rod and recorded as 90 sec. White bars represent WT and striped bars represent LXR$\beta-/-$ (n = 10–13 for each group; box: mean ± SD; whisker: min, max; *, $P < 0.01$, Student's t test). (*A*) The LXR$\beta-/-$ male mice performed better for each day as the trial went on and they learned equally as well as the WT mice, but for the male LXR$\beta-/-$ mice, the retention time to stay on the rod was significantly shorter than for WT mice for all 5 days. (*B*) Female LXR$\beta-/-$ performed as well as the WT females, and both the learning ability and retention time to stay on the rod for all of the 5 days were normal.

Female LXR$\beta-/-$ mice performed as well as did WT females (day 1: WT, 49 ± 27 sec; LXR$\beta-/-$, 49 ± 22 sec; $P = 0.989$; day 2: WT, 69 ± 23 sec; LXR$\beta-/-$, 72 ± 20 sec; $P = 0.756$; day 3: WT, 76 ± 15 sec; LXR$\beta-/-$, 70 ± 12 sec; $P = 0.501$; Day 4: WT, 90 ± 0 sec; LXR$\beta-/-$, 89 ± 2 sec; $P = 0.232$; and day 5: WT, 86 ± 8 sec; LXR$\beta-/-$, 86 ± 7 sec; $P = 0.905$). Females were also tested on the rota-rod for 2 consecutive days at the age of 9 months; however, at this age they also showed no signs of impaired motor performance (day 1: WT, 73 ± 24 sec; LXR$\beta-/-$, 80 ± 9 sec; $P = 0.410$; and day 2: WT, 85 ± 10 sec; LXR$\beta-/-$, 87 ± 5 sec; $P = 0.569$). To test whether the impaired motor coordination of male LXR$\beta-/-$ mice is a developmental defect, young LXR$\beta-/-$ males were tested at the age of 3 months for 2 consecutive days. Their motor performance was intact at this age (day 1: WT, 51 ± 18 sec; LXR$\beta-/-$, 51 ± 19 sec; $P = 0.927$; and day 2: WT, 64 ± 22 sec; LXR$\beta-/-$, 66 ± 21 sec; $P = 0.856$). The onset of the motor disability in male LXR$\beta-/-$ mice occurs between the ages of 3 and 7 months. At 7 months of age, when the motor impairment is manifested, muscle strength was tested with the wire-hanging test. LXR$\beta-/-$ males performed as well as the WT mice, indicating that muscle strength was normal (score of gripping: WT, 3 ± 1; LXR$\beta-/-$, 3 ± 1; $P = 0.737$; and latency to fall: WT, 25 ± 8 sec; LXR$\beta-/-$, 22 ± 6 sec; $P = 0.360$).

Motor Endplate Innervation. Biceps femoris muscles from 7-month-old male LXR$\beta-/-$ mice were stained for neuromuscular junctions. Tetramethylrhodamine-conjugated α-bungarotoxin was used to visualize acetylcholine receptors localized at the motor endplates, and synapsin I served as a marker for synaptic terminals from the innervating axons (Fig. 2). There was no difference between the LXR$\beta-/-$ and WT males (percent innervated motor endplates: WT, 77 ± 14%; LXR$\beta-/-$, 71 ± 10%; $P = 0.210$; $n = 10$ per genotype).

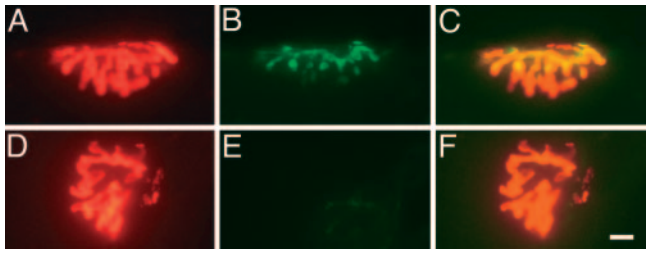

Fig. 2. Neuromuscular junction immunohistochemistry. (*A* and *D*) Motor endplates were identified with tetramethylrhodamine conjugated α-bungarotoxin (red). (*B* and *E*) Synapsin I, seen in green, was used as a marker for axon innervation. (*C*) Innervated endplate with yellow, indicating overlap of motor endplates with synapsin I staining. (*F*) Denervated endplates with no overlap of synapsin I staining. (Bar, 10 μm.)

Motor Neuron Degeneration and Astrogliosis. Nissl staining of spinal cords from 7-month-old male LXR$\beta-/-$ revealed a decrease in the number of large α motor neurons that also could be seen with Mayer's hematoxylin counterstaining (Fig. 3*A*). Staining with ChAT was used as a marker for the cholinergic motor neurons. The number of motor neurons was evaluated by counting large ChAT-positive cells, having a distinct nucleus, in the lateroventral horns of L1 segments of the spinal cord (WT, 6 ± 1 motor neurons per section; LXR$\beta-/-$, 4 ± 1 motor neurons per section; $P < 0.001$; n = 8 per genotype). Degeneration of neurons usually coincides with activation of astroglia, and as a marker for these cells we used GFAP, an intermediate filament protein found only in glial cells or cells of glial origin. The number of astrocytes was evaluated by counting GFAP-positive cells, having a distinct star-like shaped cell body in the lateroventral horns of L1 segments of the spinal cord. There were more astrocytes in the LXR$\beta-/-$ males (WT, 12 ± 2 astrocytes per section; LXR$\beta-/-$, 16 ± 3 astrocytes per section; $P = 0.004$; $n = 8$ per genotype). In addition, the astrocytes in LXR$\beta-/-$ mice appeared to be larger than those in WT mice (Fig. 3 *B*). This might indicate activation of astrocytes in male LXR$\beta-/-$ mice.

Luxol fast blue was used to stain for myelin, but no areas of demyelination could be detected in either the spinal cord (Fig. 3*A*) or brain of LXR$\beta-/-$ males. Lipid accumulation was visualized by staining with Oil red O. Lipid deposits could be detected in the motor neurons of both WT and LXR$\beta-/-$, but the size of the lipid deposits were larger in male LXR$\beta-/-$ and more deposit sites could be detected per cell (Fig. 3*C*).

Decreased Axon Size in Ventral Nerve Roots. Ventral nerve roots from L1 segments of the spinal cord were visualized by staining with 1% aqueous toluidine blue (Fig. 4). Measurement of the mean diameter of axons revealed a decrease in caliber size of 7-month-old male LXR$\beta-/-$ mice (WT, 4.1 ± 0.3 μm; LXR$\beta-/-$, 3.7 ± 0.1 μm; $P = 0.022$; $n = 5$ per genotype). The smaller caliber size of the axons in male LXR$\beta-/-$ could indicate ongoing pathologic alterations such as axonal atrophy.

Normal Morphology of Cerebellum. The cerebellum influences the motor system by adjusting the operation of motor centers in the cortex and brainstem so that the action of movement corresponds to the intention of posture. This evaluation process is important for the spatial accuracy and temporal coordination of

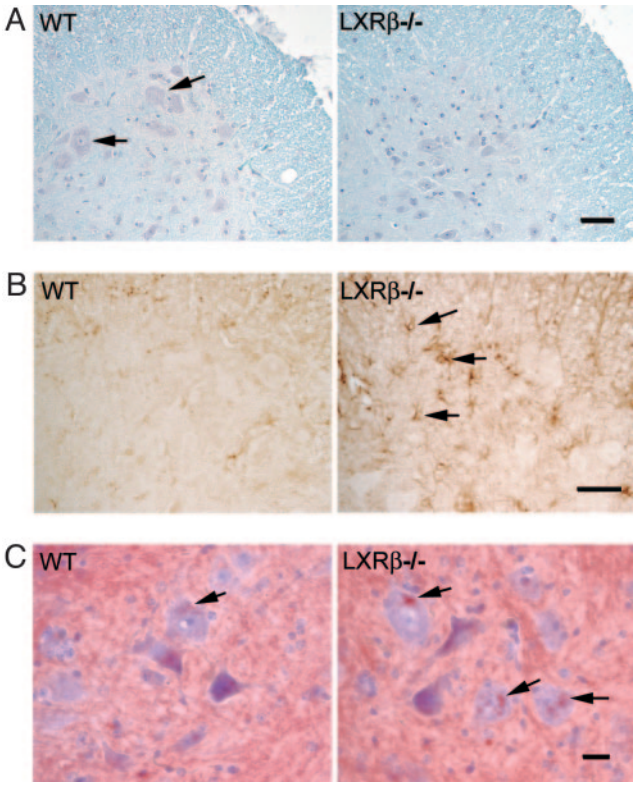

Fig. 3. Neuropathology in the lateroventral horns of L1 segments of the spinal cord in 7-month-old male mice. (*A*) Luxol fast blue was used to stain myelin, and counterstaining with Mayer's hematoxylin was performed to visualize cell nuclei. No evidence of demyelination was found in LXR$\beta-/-$ as compared with WT mice. However, loss of large α-motor neurons can be seen in the LXR$\beta-/-$ mice. Arrows indicate α-motor neurons in WT mice. The number of motor neurons was evaluated by counting large ChAT-positive cells and this count gave 6 $\pm$ 1 motor neurons per section for WT and 4 $\pm$ 1 motor neurons per section for LXR$\beta-/-$ mice, $P < 0.001$; Student's *t* test; $n = 8$ per genotype. Note that the picture only shows one of the two ventral horns in a section. (Bar, 50 μm.) (*B*) GFAP staining of astroglia can be seen as brown star-like shaped cell bodies, as indicated with arrows in LXR$\beta-/-$ sample. More activated astrocytes with large cell bodies can be seen in LXR$\beta-/-$ mice as compared with WT. Counting the number of GFAP-positive cells gave 12 $\pm$ 2 astrocytes per section for WT and 16 $\pm$ 3 astrocytes per section for LXR$\beta-/-$ mice; $P = 0.004$; Student's *t* test; $n = 8$ per genotype. Note that the picture only shows one of the two ventral horns in a section. (Bar, 50 μm.) (*C*) Lipid deposits were revealed by staining with Oil red O, as indicated by arrows. More and lager deposits can be seen in motor neurons of LXR$\beta-/-$ mice compared with WT mice; $n = 5$ per genotype. (Bar, 20 μm.)

movements. Nissl staining of cerebellum did not reveal any morphological differences in 7-month-old LXR$\beta-/-$ male mice (data not shown). Calbindin was used as a marker for Purkinje cells. Both calbindin and calretinin, which are expressed by granule cells, belong to the large family of EF-hand calcium-binding proteins and are modulators of intracellular calcium transients. Knockouts of calbindin and calretinin have shown that these calcium-buffering proteins are critical for the precision of motor coordination (22, 23). No difference in the number of large calbindin-positive cells could be detected in male LXR$\beta-/-$ as compared with WT mice (data not shown). On Western blots of cerebellar extracts, with α-tubulin used as a loading control, no difference in expression of either calbindin or calretinin could be detected between male LXR$\beta-/-$ and WT mice (Fig. 5).

Discussion

We report here that the absence of LXRβ in male mice causes a selective vulnerability of large motor neurons. At 7 months of age, these mice exhibit impaired performance on the rota-rod and this impairment is associated with lipid accumulation and loss of motor neurons in the spinal cord, together with axonal atrophy and astrogliosis. Several of these features are reminiscent of the neuropathological signs of chronic motor neuron disease such as ALS.

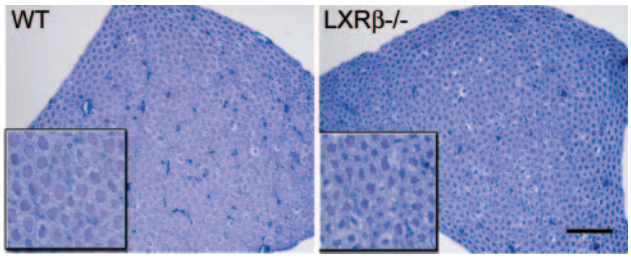

Fig. 4. Toluidine blue staining of L1 ventral nerve roots. The size of the axon calibers is smaller in LXR$\beta-/-$ mice as compared with WT, perhaps indicating axonal atrophy. Measurement of the mean diameter gave 4.1 $\pm$ 0.3 μm for WT and 3.7 $\pm$ 0.1 μm for LXR$\beta-/-$ mice; $P = 0.022$; Student's *t* test; $n = 5$ per genotype. (*Insets*) Higher magnification of selected parts can be seen. (Bar, 50 μm.)

The impaired motor coordination in male LXR$\beta-/-$ mice is an age-related phenomenon and is not evident when mice are 3 months old. The onset of disability occurs between the ages of 3 and 7 months. At 7 months of age, when the motor impairment is manifested, LXR$\beta-/-$ males perform as well as the WT mice in the wire-hanging test, which is an indication that muscle strength is still normal. At this age, there is also normal innervation of motor endplates in the biceps femoris muscles. However, the mean diameter of axons in the ventral nerve roots of the spinal cord is decreased in 7-month-old male LXR$\beta-/-$ mice. This decrease in caliber of the axons could indicate ongoing pathologic alterations of the larger axons in the ventral nerve root, which could lead to reduced control over muscle action and a motor coordination problem, as is seen in LXR$\beta-/-$ males.

Similar alterations are seen in ALS patients, where there appears to be a selective degeneration of α motor neurons with large axonal diameters, whereas motor neurons with small axonal calibers (γ motor neurons) are spared (24, 25). Axonal

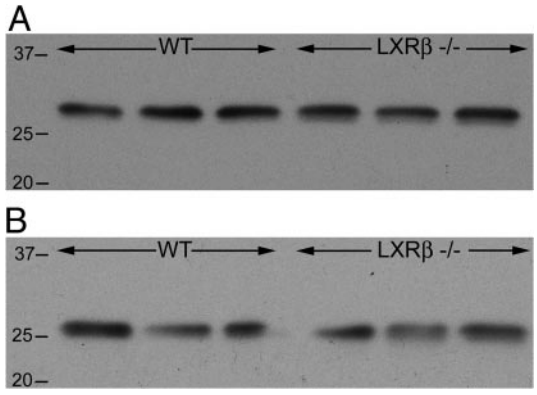

Fig. 5. Western blot of cerebellar extract from 7-month-old male mice. No difference in protein expression of either of the two calcium-buffering proteins, calretinin or calbindin, could be detected in LXR$\beta-/-$ mice as compared with WT. Size ladder is indicated on the left. α-tubulin (66 kDa) was used as a loading control ($n = 3$ for each genotype). (*A*) The protein expression of calretinin ($\approx$30 kDa), mainly produced by granule cells in the cerebellum, did not differ in LXR$\beta-/-$ mice compared with WT. (*B*) The protein expression of calbindin (28 kDa), mainly produced by Purkinje cells in the cerebellum, did not differ in LXR$\beta-/-$ mice compared with WT.

atrophy and loss of large fibers is also reported to be associated with aging (26, 27). Reduction in the rate of axonal transport of various materials occurs with increasing age, and the reduced transport of microtubule and neurofilament proteins could lead to difficulties in maintaining the cytoskeletal framework, thereby leading to axonal atrophy or fiber loss (28, 29). One hypothesis for the selective vulnerability of motor neurons in ALS is a high content of neurofilament proteins and large calibers of axons.

The male-specific motor impairment that we report in the present study is in line with the clinical findings of ALS. In the sporadic form of ALS, the majority of affected patients are men, suggesting that not-yet-identified genetic or hormonal factors could play a role in the pathogenesis. However, this difference in incidence between the sexes may diminish with aging, because women get the disease later in life than men (30). Such epidemiological evidence raises the possibility that estrogen may have a neuroprotective role in ALS. Potential neuroprotective mechanisms for estrogen include enhancing neurotrophin release, interactions with neurotransmitters, and providing antioxidant benefit (31). Estrogen also suppresses lipid peroxidation, which is known to impair the function of plasma membrane ATPases and glucose- and glutamate transporters, that in turn may lead to membrane depolarization, reduced energy availability, and increased extracellular glutamate levels (32, 33).

ALS is epidemiologically subclassified into sporadic (90–95%) and familial (5–10%) cases. The etiology of sporadic ALS is unknown. Twenty percent of familial ALS, where the disease is inherited in an autosomal dominant manner, is caused by missense mutations in the antioxidant enzyme Cu/Zn superoxide dismutase I (SOD1), an oxidoreductase that catalyzes the reaction between superoxide anions and hydrogen to yield molecular oxygen and hydrogen peroxide (34). The cause of motor neuron degeneration was first thought to be reduced enzymatic activity as a consequence of the SOD1 gene mutations, but several mutations identified in ALS patients leave SOD1 activity intact and others may even enhance enzyme catalytic function (35). SOD1 knockout mice do not develop spontaneous motor neuron disease, whereas transgenic mice expressing mutant SOD1 develop paralysis, despite possessing two normal SOD1 alleles (36). These data suggest that the disease results from the gain of some cytotoxic function rather than loss of dismutase activity.

SOD1 gene mutations are less frequent in sporadic ALS cases (2.6%), and the fact that only a subset of cases can be linked to one particular molecular defect suggests that the etiology of motor neuron diseases is likely to be multifactorial. A complex interplay between genetic factors, oxidative stress, glutaminergic excitotoxicity, impaired mitochondrial function, and aberrant protein aggregation has been suggested (37).

Because the LXRs are important for transport, catabolism, and efflux of cholesterol, we speculate that pathological accumulation of lipids could predispose motor neurons to degeneration. The size of the lipid deposits in motor neurons is larger in LXR$\beta-/-$ males, and more deposit sites could be detected per cell than in WT mice. One report has shown increased levels of sphingomyelin, ceramides, and cholesterol esters in the spinal cords of ALS patients and transgenic mice with mutation of the SOD1, suggesting that these abnormalities can sensitize motor neurons to programmed cell death (38).

LXRs have been shown to enhance the release of cholesterol from cultured primary murine astrocytes by increasing the expression of ATP-binding cassette transporter A1 (39). However, little or no effect was seen with the LXR agonist on either cholesterol efflux or LXR target gene expression in primary neuronal cultures. These findings are in consonance with the mechanistic model, suggested by Pfrieger (40), of a net export of cholesterol from astrocytes to neurons that is feedback-regulated with participation of LXRβ, ATP-binding cassette transporter A1, CYP46A1, and 24(S)-hydroxycholesterol. However, the relative importance of different lipoproteins and their receptors for the transport and recycling of cholesterol within the CNS is still unknown. It is possible that only specific types of neurons depend on external cholesterol. Cholesterol homeostasis throughout the brain is not uniform, and the expression of enzymes involved in the cholesterol metabolism differs from region to region (41, 42).

The spinal cord has a high tissue concentration of cholesterol and a high rate of cholesterol synthesis that probably represents a high content of white matter with compact myelin produced by oligodendrocytes (18). However, neuronal CYP46A1 is less abundant in the spinal cord than in the brain, and presumably, mechanisms other than 24-hydroxylation of cholesterol are important for cholesterol excretion from the spinal cord (19). In mice with a deletion of the CYP46A1, cholesterol homeostasis in the CNS is maintained by decreasing the *de novo* synthesis of cholesterol. Such a compensatory mechanism is not seen in the spinal cord of these mice, and yet there is no increase in the cholesterol content of the tissue (17). This finding suggests that the cholesterol efflux from the spinal cord does not occur through conversion of cholesterol to 24(S)-hydroxycholesterol, but rather, by some other not-yet-identified transport mechanism.

One of the possible transport mechanisms that have been suggested for cholesterol efflux from the CNS is the ATP-binding cassette transporters G5 and G8 (ABCG5/G8) route. So far, the major role for ABCG5/G8 is thought to be in the enterohepatic sterol transport where the absorption of dietary cholesterol is controlled through efflux back into the lumen of the gut. The response of ABCG5 and ABCG8 to cholesterol requires the LXRs and treatment with a synthetic LXR agonist increases the sterol excretion by the ABCG5/G8 route *in vivo* (43). Mutation in either of these transporters causes sitosterolemia, a rare recessive disorder with patients accumulating plant- and shellfish-derived sterols from the diet in the blood and tissues (44, 45). Plant sterols have been reported to accumulate in the brain of ABCG5- and ABCG8-deficient mice, although the extent of the accumulation was much lower than in the liver and plasma (46). However, some plant sterols have been suggested to be neurotoxic and to be the cause of the ALS-parkinsonism dementia complex found among the population of Guam (47).

In LXR$\beta-/-$ mice, accumulation of sterols and lipids in motor neurons of the spinal cord could be due to decrease of the ABC transporters, such as A1, G5, and G8, which previously have been shown to be controlled by LXRs (48–50). We have shown that the expression of several ABC transporters is impaired in the brains of LXR$\alpha\beta$ double-knockout mice (11). LXRs may be required to drain excess sterols and lipids from the CNS, and their malfunction may cause degeneration because of sterol overload.

Defective cholesterol homeostasis is also the cause of Niemann–Pick type C disease, a neurodegenerative disease characterized by degeneration of axons and dendrites, and ultimately, loss of neurons, particularly cerebellar Purkinje cells (51). Niemann–Pick type C disease is an autosomal recessive disorder, and the cause is abnormal intracellular trafficking of cholesterol (52, 53). On the basis of the data presented in our study, we suggest that chronic motor neuron diseases can be added to the list of neurodegenerative diseases associated with defective cholesterol homeostasis.

We thank C. Thulin-Andersson for excellent technical assistance and O. Imamov for helpful discussions and assistance with the IMAGEPRO PLUS software. This work was supported by grants from The Swedish Research Council and KaroBio AB Sweden.

1. Alberti, S., Steffensen, K. R. & Gustafsson, J. A. (2000) *Gene* **243,** 93–103.
2. Janowski, B. A., Willy, P. J., Devi, T. R., Falck, J. R. & Mangelsdorf, D. J. (1996) *Nature* **383,** 728–731.
3. Lehmann, J. M., Kliewer, S. A., Moore, L. B., Smith-Oliver, T. A., Oliver, B. B., Su, J. L., Sundseth, S. S., Winegar, D. A., Blanchard, D. E., Spencer, T. A. & Willson, T. M. (1997) *J. Biol. Chem.* **272,** 3137–3140.
4. Forman, B. M., Ruan, B., Chen, J., Schroepfer, G. J., Jr., & Evans, R. M. (1997) *Proc. Natl. Acad. Sci. USA* **94,** 10588–10593.
5. Janowski, B. A., Grogan, M. J., Jones, S. A., Wisely, G. B., Kliewer, S. A., Corey, E. J. & Mangelsdorf, D. J. (1999) *Proc. Natl. Acad. Sci. USA* **96,** 266–271.
6. Fu, X., Menke, J. G., Chen, Y., Zhou, G., MacNaul, K. L., Wright, S. D., Sparrow, C. P. & Lund, E. G. (2001) *J. Biol. Chem.* **276,** 38378–38387.
7. Peet, D. J., Turley, S. D., Ma, W., Janowski, B. A., Lobaccaro, J. M., Hammer, R. E. & Mangelsdorf, D. J. (1998) *Cell* **93,** 693–704.
8. Alberti, S., Schuster, G., Parini, P., Feltkamp, D., Diczfalusy, U., Rudling, M., Angelin, B., Bjorkhem, I., Pettersson, S. & Gustafsson, J. A. (2001) *J. Clin. Invest.* **107,** 565–573.
9. Kainu, T., Kononen, J., Enmark, E., Gustafsson, J. A. & Pelto-Huikko, M. (1996) *J. Mol. Neurosci.* **7,** 29–39.
10. Annicotte, J. S., Schoonjans, K. & Auwerx, J. (2004) *Anat. Rec.* **277A,** 312–316.
11. Wang, L., Schuster, G. U., Hultenby, K., Zhang, Q., Andersson, S. & Gustafsson, J. A. (2002) *Proc. Natl. Acad. Sci. USA* **99,** 13878–13883.
12. Edmond, J., Korsak, R. A., Morrow, J. W., Torok-Both, G. & Catlin, D. H. (1991) *J. Nutr.* **121,** 1323–1330.
13. Jurevics, H. & Morell, P. (1995) *J. Neurochem.* **64,** 895–901.
14. Reese, T. S. & Karnovsky, M. J. (1967) *J. Cell Biol.* **34,** 207–217.
15. Lutjohann, D., Breuer, O., Ahlborg, G., Nennesmo, I., Siden, A., Diczfalusy, U. & Bjorkhem, I. (1996) *Proc. Natl. Acad. Sci. USA* **93,** 9799–9804.
16. Lund, E. G., Xie, C., Kotti, T., Turley, S. D., Dietschy, J. M. & Russell, D. W. (2003) *J. Biol. Chem.* **278,** 22980–22988.
17. Xie, C., Lund, E. G., Turley, S. D., Russell, D. W. & Dietschy, J. M. (2003) *J. Lipid Res.* **44,** 1780–1789.
18. Quan, G., Xie, C., Dietschy, J. M. & Turley, S. D. (2003) *Brain Res. Dev. Brain Res.* **146,** 87–98.
19. Lund, E. G., Guileyardo, J. M. & Russell, D. W. (1999) *Proc. Natl. Acad. Sci. USA* **96,** 7238–7243.
20. Nicoletti, A., Kaveri, S., Caligiuri, G., Bariety, J. & Hansson, G. K. (1998) *J. Clin. Invest.* **102,** 910–918.
21. West, M. J., Slomianka, L. & Gundersen, H. J. (1991) *Anat. Rec.* **231,** 482–497.
22. Schiffmann, S. N., Cheron, G., Lohof, A., d'Alcantara, P., Meyer, M., Parmentier, M. & Schurmans, S. (1999) *Proc. Natl. Acad. Sci. USA* **96,** 5257–5262.
23. Airaksinen, M. S., Eilers, J., Garaschuk, O., Thoenen, H., Konnerth, A. & Meyer, M. (1997) *Proc. Natl. Acad. Sci. USA* **94,** 1488–1493.
24. Kawamura, Y., Dyck, P. J., Shimono, M., Okazaki, H., Tateishi, J. & Doi, H. (1981) *J. Neuropathol. Exp. Neurol.* **40,** 667–675.
25. Sobue, G., Matsuoka, Y., Mukai, E., Takayanagi, T. & Sobue, I. (1981) *J. Neurol. Sci.* **50,** 413–421.
26. Low, P. A. & Dyck, P. J. (1977) *Acta Neuropathol.* **40,** 219–225.
27. Kawamura, Y., Okazaki, H., O'Brien, P. C. & Dych, P. J. (1977) *J. Neuropathol. Exp. Neurol.* **36,** 853–860.
28. McMartin, D. N. & O'Connor, J. A., Jr. (1979) *Mech. Ageing Dev.* **10,** 241–248.
29. Komiya, Y. (1980) *Brain Res.* **183,** 477–480.
30. Meininger, V., Bensimon, G. & Lacomblez, L. (1995) in *Advances of Neurology*, eds. Ferratrice, G. & Munset, T. (Lippincott Raven, Philadelphia), pp. 199–207.
31. Henderson, V. W. (1997) *Am. J. Med.* **103,** 11S–18S.
32. Goodman, Y., Bruce, A. J., Cheng, B. & Mattson, M. P. (1996) *J. Neurochem.* **66,** 1836–1844.
33. Mattson, M. P. (1998) *Trends Neurosci.* **21,** 53–57.
34. Rosen, D. R., Siddique, T., Patterson, D., Figlewicz, D. A., Sapp, P., Hentati, A., Donaldson, D., Goto, J., O'Regan, J. P. & Deng, H. X. (1993) *Nature* **362,** 59–62.
35. Robberecht, W. (2000) *J. Neurol.* **247,** 2–6.
36. Reaume, A. G., Elliott, J. L., Hoffman, E. K., Kowall, N. W., Ferrante, R. J., Siwek, D. F., Wilcox, H. M., Flood, D. G., Beal, M. F., Brown, R. H., Jr., *et al.* (1996) *Nat. Genet.* **13,** 43–47.
37. Cleveland, D. W. & Rothstein, J. D. (2001) *Nat. Rev. Neurosci.* **2,** 806–819.
38. Cutler, R. G., Pedersen, W. A., Camandola, S., Rothstein, J. D. & Mattson, M. P. (2002) *Ann. Neurol.* **52,** 448–457.
39. Whitney, K. D., Watson, M. A., Collins, J. L., Benson, W. G., Stone, T. M., Numerick, M. J., Tippin, T. K., Wilson, J. G., Winegar, D. A. & Kliewer, S. A. (2002) *Mol. Endocrinol.* **16,** 1378–1385.
40. Pfrieger, F. W. (2003) *BioEssays* **25,** 72–78.
41. Runquist, M., Parmryd, I., Thelin, A., Chojnacki, T. & Dallner, G. (1995) *J. Neurochem.* **65,** 2299–2306.
42. Bae, S. H., Lee, J. N., Fitzky, B. U., Seong, J. & Paik, Y. K. (1999) *J. Biol. Chem.* **274,** 14624–14631.
43. Yu, L., York, J., von Bergmann, K., Lutjohann, D., Cohen, J. C. & Hobbs, H. H. (2003) *J. Biol. Chem.* **278,** 15565–15570.
44. Salen, G., Horak, I., Rothkopf, M., Cohen, J. L., Speck, J., Tint, G. S., Shore, V., Dayal, B., Chen, T. & Shefer, S. (1985) *J. Lipid Res.* **26,** 1126–1133.
45. Gregg, R. E., Connor, W. E., Lin, D. S. & Brewer, H. B., Jr. (1986) *J. Clin. Invest.* **77,** 1864–1872.
46. Yu, L., von Bergmann, K., Lutjohann, D., Hobbs, H. H. & Cohen, J. C. (2004) *J. Lipid Res.* **45,** 301–307.
47. Khabazian, I., Bains, J. S., Williams, D. E., Cheung, J., Wilson, J. M., Pasqualotto, B. A., Pelech, S. L., Andersen, R. J., Wang, Y. T., Liu, L., *et al.* (2002) *J. Neurochem.* **82,** 516–528.
48. Schwartz, K., Lawn, R. M. & Wade, D. P. (2000) *Biochem. Biophys. Res. Commun.* **274,** 794–802.
49. Venkateswaran, A., Laffitte, B. A., Joseph, S. B., Mak, P. A., Wilpitz, D. C., Edwards, P. A. & Tontonoz, P. (2000) *Proc. Natl. Acad. Sci. USA* **97,** 12097–12102.
50. Repa, J. J., Berge, K. E., Pomajzl, C., Richardson, J. A., Hobbs, H. & Mangelsdorf, D. J. (2002) *J. Biol. Chem.* **277,** 18793–18800.
51. March, P. A., Thrall, M. A., Brown, D. E., Mitchell, T. W., Lowenthal, A. C. & Walkley, S. U. (1997) *Acta Neuropathol.* **94,** 164–172.
52. Loftus, S. K., Morris, J. A., Carstea, E. D., Gu, J. Z., Cummings, C., Brown, A., Ellison, J., Ohno, K., Rosenfeld, M. A., Tagle, D. A., *et al.* (1997) *Science* **277,** 232–235.
53. Naureckiene, S., Sleat, D. E., Lackland, H., Fensom, A., Vanier, M. T., Wattiaux, R., Jadot, M. & Lobel, P. (2000) *Science* **290,** 2298–2301.